"Two kinematical classes of CMEs observed by *SDO*/AIA, *PROBA2*/SWAP, and coronographs on board *SOHO* and *STEREO*"

Ewa Chmielewska, Michał Tomczak

PROBA2 was launched on a Rockot launcher from the Russian launch base Plesetsk, on November 2 2009.

PROBA2 carries two solar instruments (SWAP and LYRA) and two instruments to study the space environment surrounding the spacecraft (DSLP and TPMU).

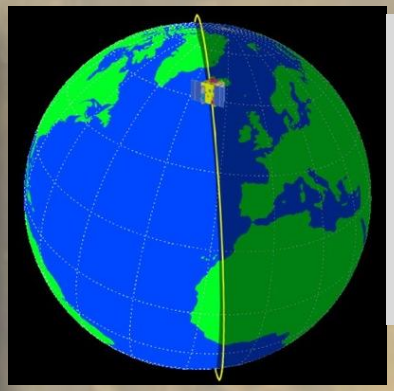

PROBA2 follows a sun-synchronous orbit. This means that PROBA2's orbit will track the terminator, following the dividing line between day and night on earth over the poles as in the figure on the left.

General overview of the SWAP optical path

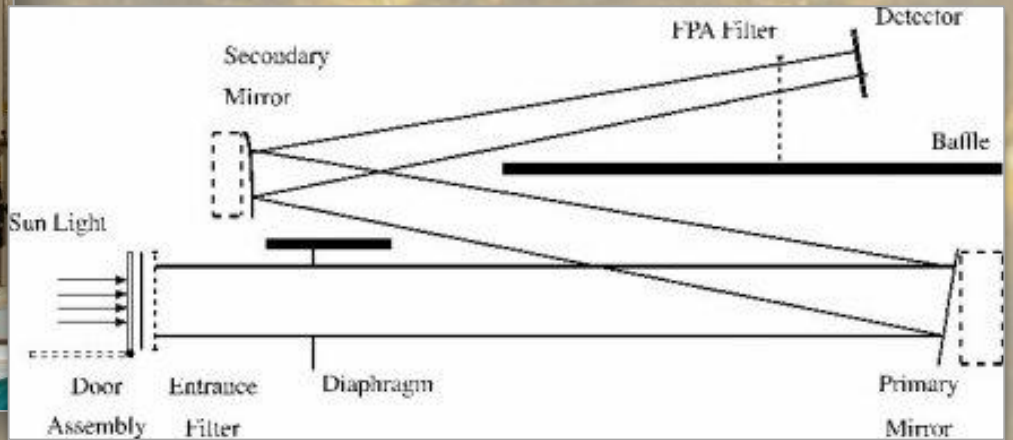

SWAP (**S**un **W**atcher using **A**ctive Pixel System detector and Image **P**rocessing) is a small EUV telescope that images the solar corona with a bandpass around 17.4 nm, corresponding to a temperature of 1 million degrees.

- ❑Image cadence---typically 130 seconds
- ❑Provides data over 54x54 arcmin FoV with 3.17 arcsec pixels
- ❑CMOS-APS technology

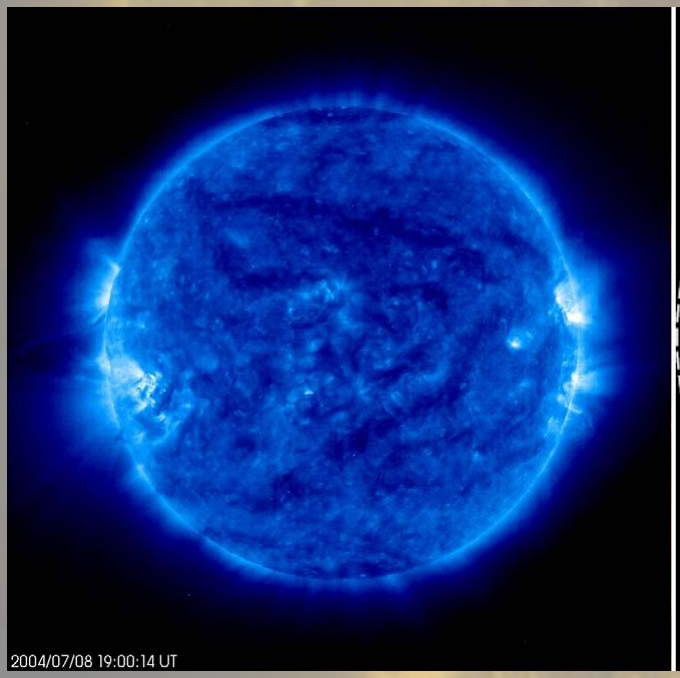

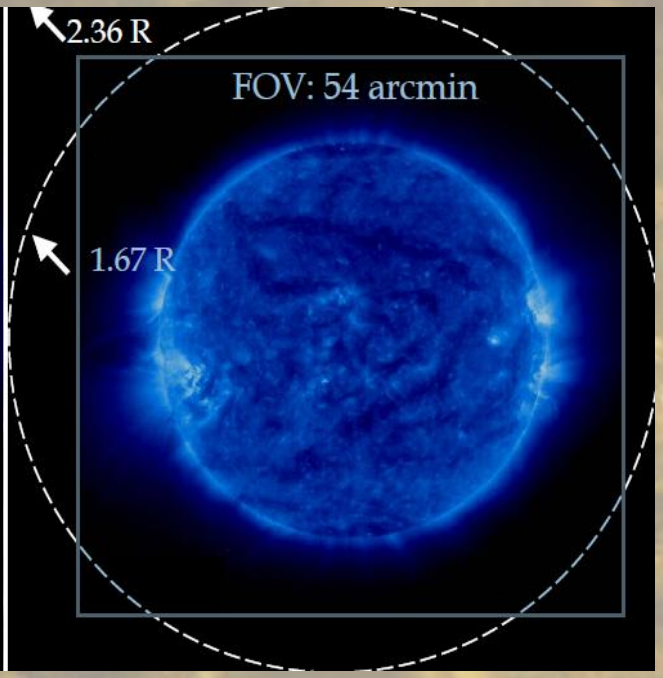

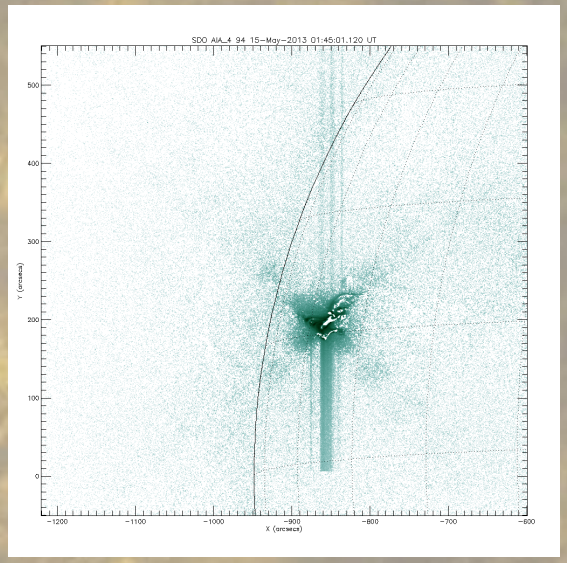

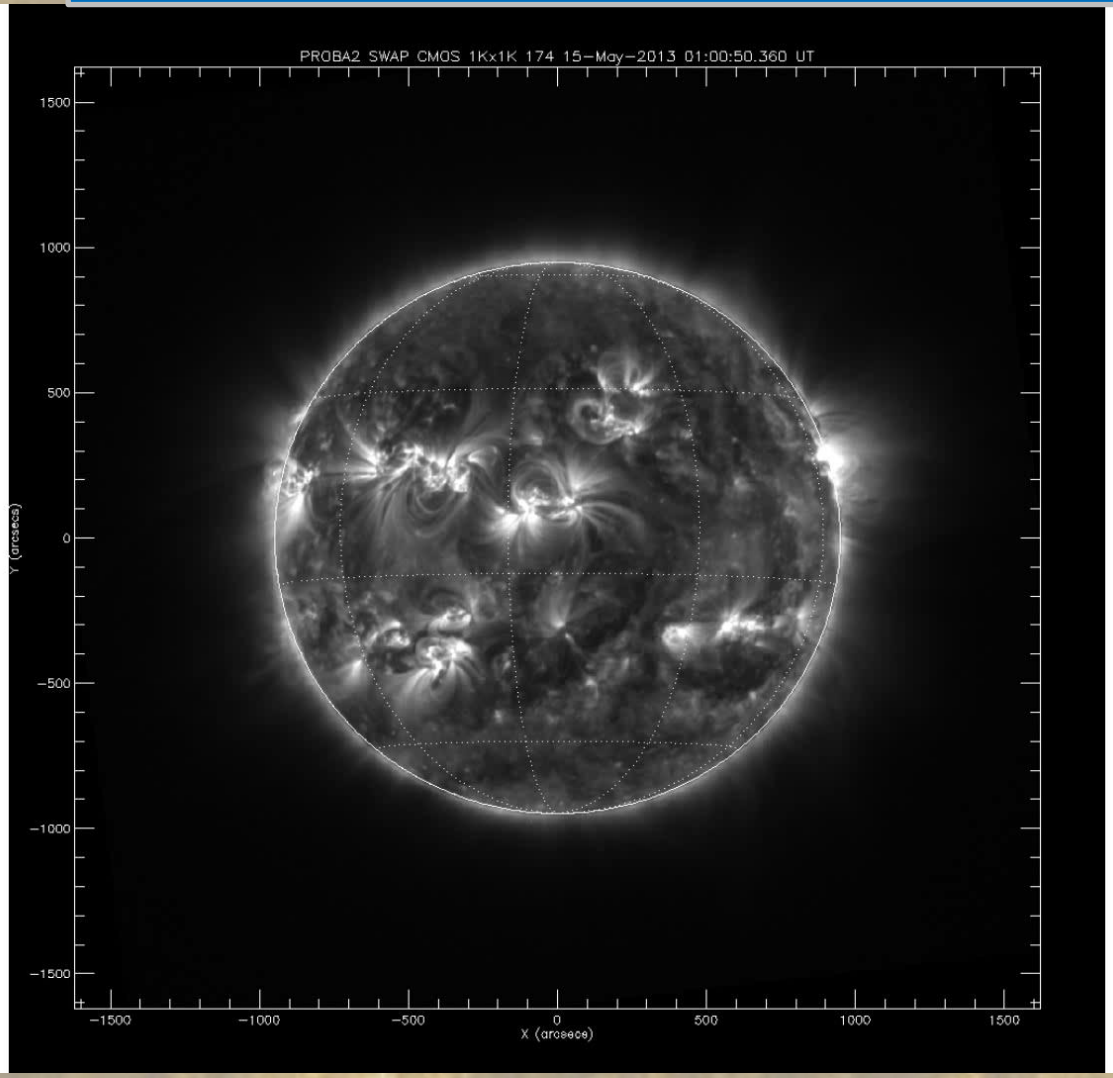
PROBA2 SWAP CMOS 1Kx1K 174 15-May-2013 01:00:50.360 UT
1500
1000
500
0
-500
-1000
-1500
Y (arcsecs)
-1500
-1000
-500
0
500
1000
1500
X (arcsecs)

Are there really two kinematical types of CMEs ?

Gosling et al., 1976, Solar Phys., 48, 398-397;

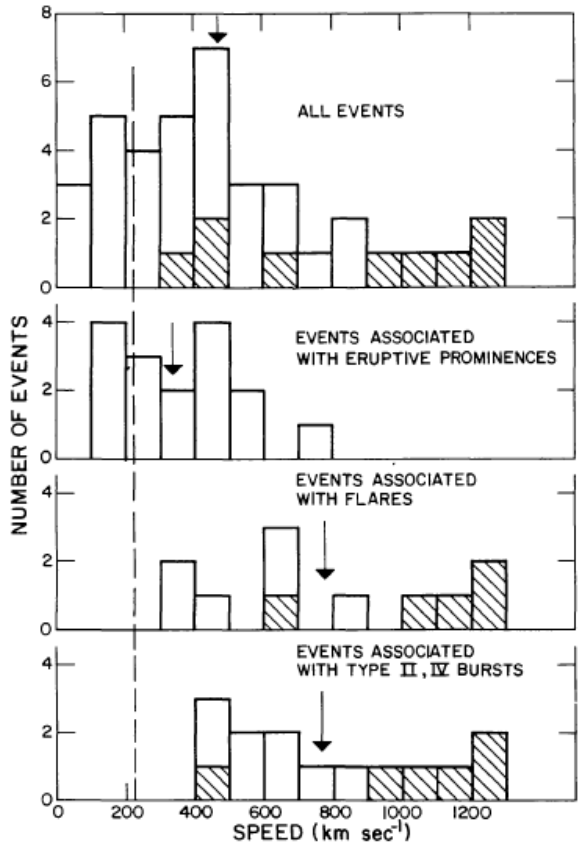

The number distribution of measured speeds of the leading edges of CME.

Moon et al., 2002, Astrophys. J., 581, 694-702;

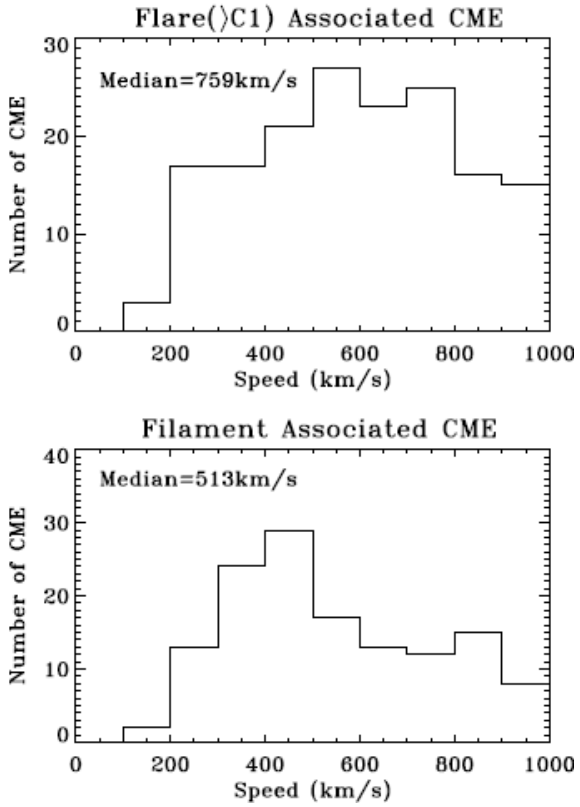

Histograms for the CME speeds corrected for the projection effect: flare (>C1)-associated CMEs (upper panel) and eruptive-filament–associated events (lower panel).

Vršnak i in, 2005, Astron. Astrophys., 435,1149-1157

The statistical analysis of 545 flare-associated CMEs and 104 non-flare CMEs observed in the heliocentric distance range 2–30 $R_{\odot}$.

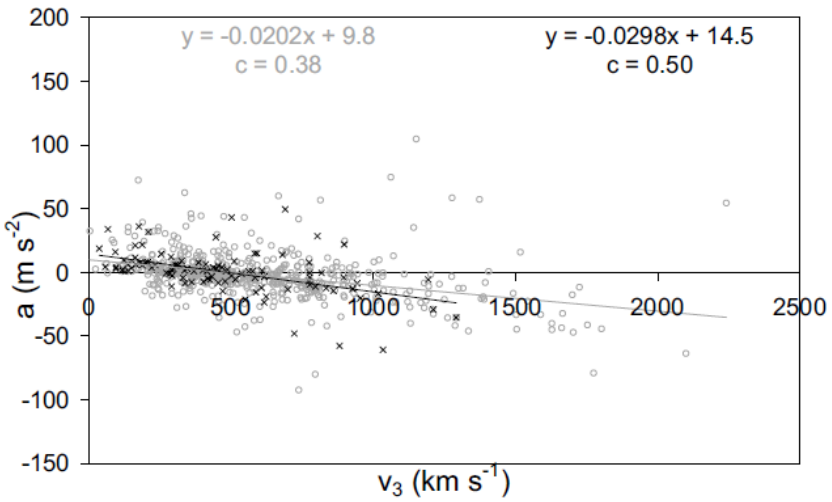

The acceleration-velocity relationship, a(v3), of the F-CMEs (gray) and non-flare CMEs (**black**).

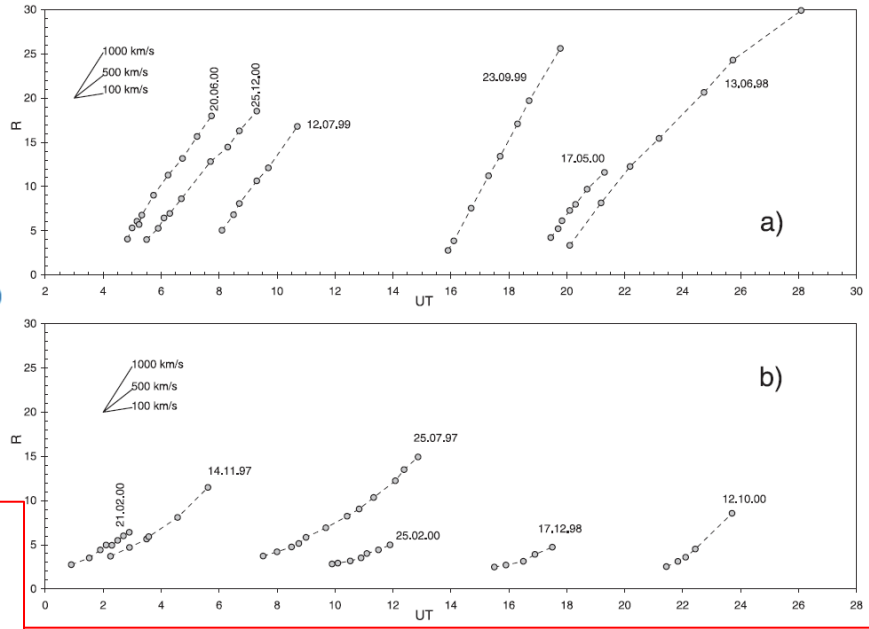

(a) Several examples of fast non-flare CMEs that show no acceleration, or even decelerate.
(b) Several examples of flare-associated CMEs showing a significant acceleration. The slopes of 100, 500, and 1000 km s^{-1} are indicated in the upper-left corner of both graphs.

	Ion	λ Å	T_p[a] K	Fraction of total emission CH	QS	AR	FL
211 Å	Cr IX	210.61	5.95	0.07	–	–	–
	Ca XVI	208.60	6.7	–	–	–	0.09
	Fe XVII	204.67	6.6	–	–	–	0.07
	Fe XIV	211.32	6.3	–	0.13	0.39	0.12
	Fe XIII	202.04	6.25	–	0.05	–	–
	Fe XIII	203.83	6.25	–	–	0.07	–
	Fe XIII	209.62	6.25	–	0.05	0.05	–
	Fe XI	209.78	6.15	0.11	0.12	–	–
	Fe X	207.45	6.05	0.05	0.03	–	–
	Ni XI	207.92	6.1	0.03	–	–	–
	Cont.			0.08	0.04	0.07	0.41
304 Å	He II	303.786	4.7	0.33	0.32	0.27	0.29
	He II	303.781	4.7	0.66	0.65	0.54	0.58
	Ca XVIII	302.19	6.85	–	–	–	0.05
	Si XI	303.33	6.2	–	–	0.11	–
	Cont.			–	–	–	–
335 Å	Al X	332.79	6.1	0.05	0.11	–	–
	Mg VIII	335.23	5.9	0.11	0.06	–	–
	Mg VIII	338.98	5.9	0.11	0.06	–	–
	Si IX	341.95	6.05	0.03	0.03	–	–
	Si VIII	319.84	5.95	0.04	–	–	–
	Fe XVI	335.41	6.45	–	–	0.86	0.81
	Fe XIV	334.18	6.3	–	0.04	0.04	–
	Fe X	184.54	6.05	0.13	0.15	–	-
	Cont.			0.08	0.05	–	0.06

	Ion	λ Å	T_p[a] K	Fraction of total emission CH	QS	AR	FL
94 Å	Mg VIII	94.07	5.9	0.03	–	–	–
	Fe XX	93.78	7.0	–	–	–	0.10
	Fe XVIII	93.93	6.85	–	–	0.74	0.85
	Fe X	94.01	6.05	0.63	0.72	0.05	–
	Fe VIII	93.47	5.6	0.04	–	–	–
	Fe VIII	93.62	5.6	0.05	–	–	–
	Cont.			0.11	0.12	0.17	–
131 Å	O VI	129.87	5.45	0.04	0.05	–	–
	Fe XXIII	132.91	7.15	–	–	–	0.07
	Fe XXI	128.75	7.05	–	–	–	0.83
	Fe VIII	130.94	5.6	0.30	0.25	0.09	–
	Fe VIII	131.24	5.6	0.39	0.33	0.13	–
	Cont.			0.11	0.20	0.54	0.04
171 Å	Ni XIV	171.37	6.35	–	–	0.04	–
	Fe X	174.53	6.05	–	0.03	–	–
	Fe IX	171.07	5.85	0.95	0.92	0.80	0.54
	Cont.			–	–	–	0.23
193 Å	O V	192.90	5.35	0.03	–	–	–
	Ca XVII	192.85	6.75	–	–	–	0.08
	Ca XIV	193.87	6.55	–	–	0.04	–
	Fe XXIV	192.03	7.25	–	–	-	0.81
	Fe XII	195.12	6.2	0.08	0.18	0.17	–
	Fe XII	193.51	6.2	0.09	0.19	0.17	–
	Fe XII	192.39	6.2	0.04	0.09	0.08	–
	Fe XI	188.23	6.15	0.09	0.10	0.04	–
	Fe XI	192.83	6.15	0.05	0.06	–	–
	Fe XI	188.30	6.15	0.04	0.04	–	–
	Fe X	190.04	6.05	0.06	0.04	–	–
	Fe IX	189.94	5.85	0.06	–	–	–
	Fe IX	188.50	5.85	0.07	–	–	–
	Cont.			–	–	0.05	0.04

O'Dwyer et al., A&A, 521, A21, 2010

CME associated with flares

We observed that **CMEs associated with flares in the SDO/AIA field of view have two phases of kinematical evolution**: slow rise and an impulsive acceleration whereas in LASCO/C2 field of view the front of CME **moves with constant speed or slightly decreases**.

the kinematical scenario described by Zhang et al., 2001

Estimated time of **onset impulsive acceleration phase for our sample coincides with start of associated flare** (Cheng et al. 2013b).

We identified **hot structures** in the high temperature passbands of the AIA, **before the impulsive acceleration phase of the eruption**.

The **velocities of the F-CMEs** and of the **NF-CMEs speeds (with hot structure or post EUV-loops)** have **similiar values**.

For CME-flares pairs we observed that **front of eruption moves with the highest speeds.**

15 maja 2013-

an expanding system of loops associated with CME, and X1.2 flare (AR 11748- N11E49) that peaked at 01:48 UT

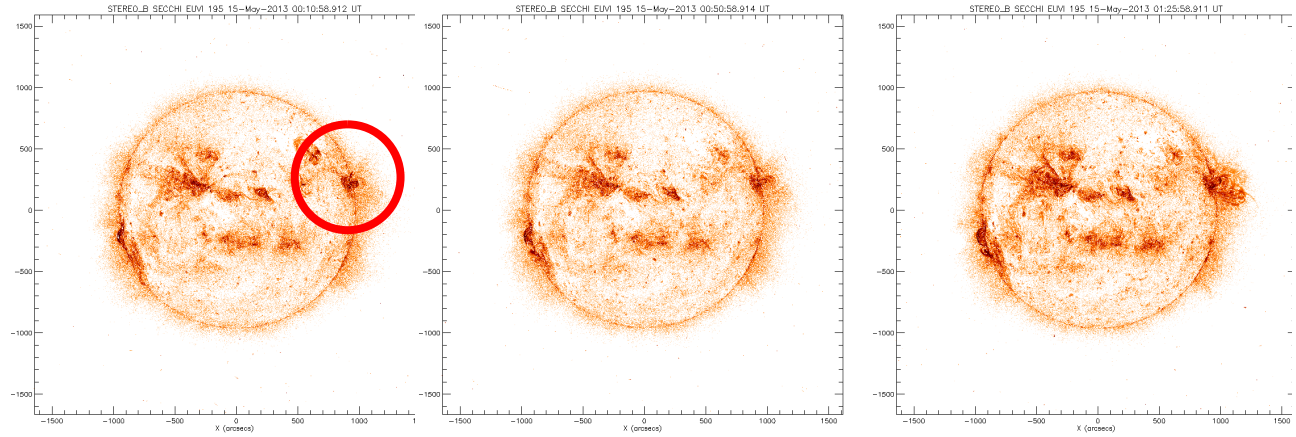

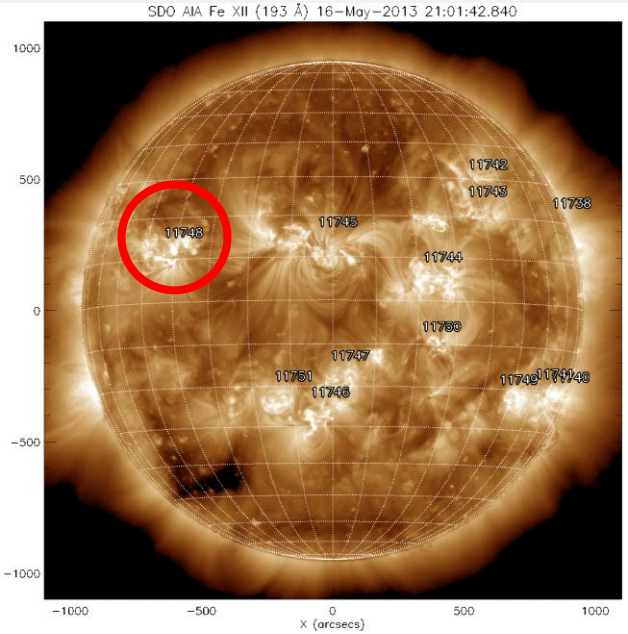

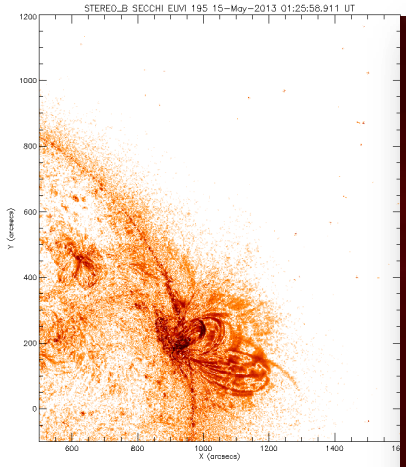

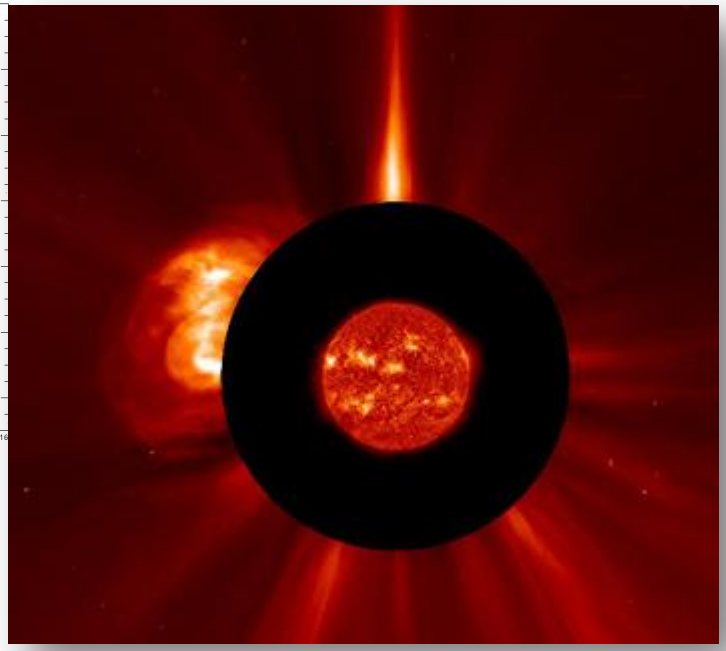

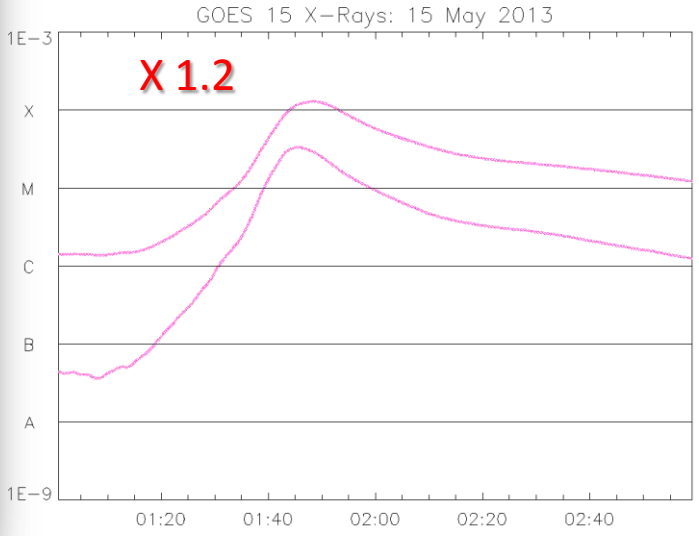

15 May 2013- the sources of hard X-ray in two ranges of energy, located at the top of the structures observed in the filter 131 Å

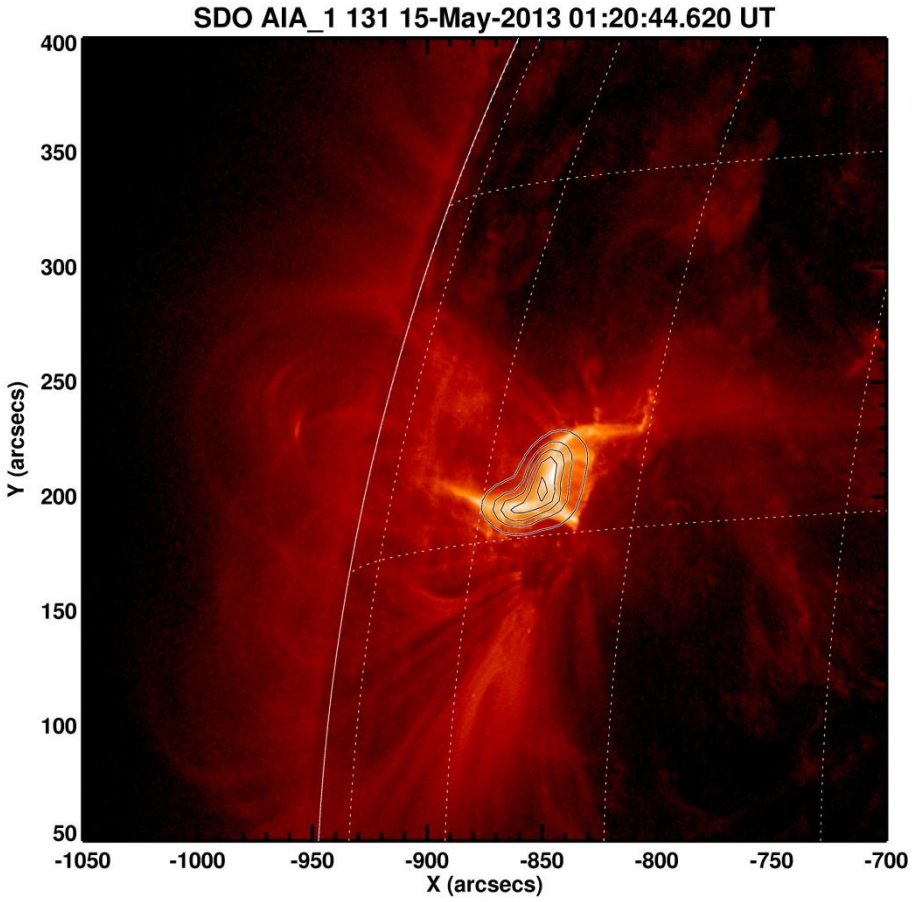

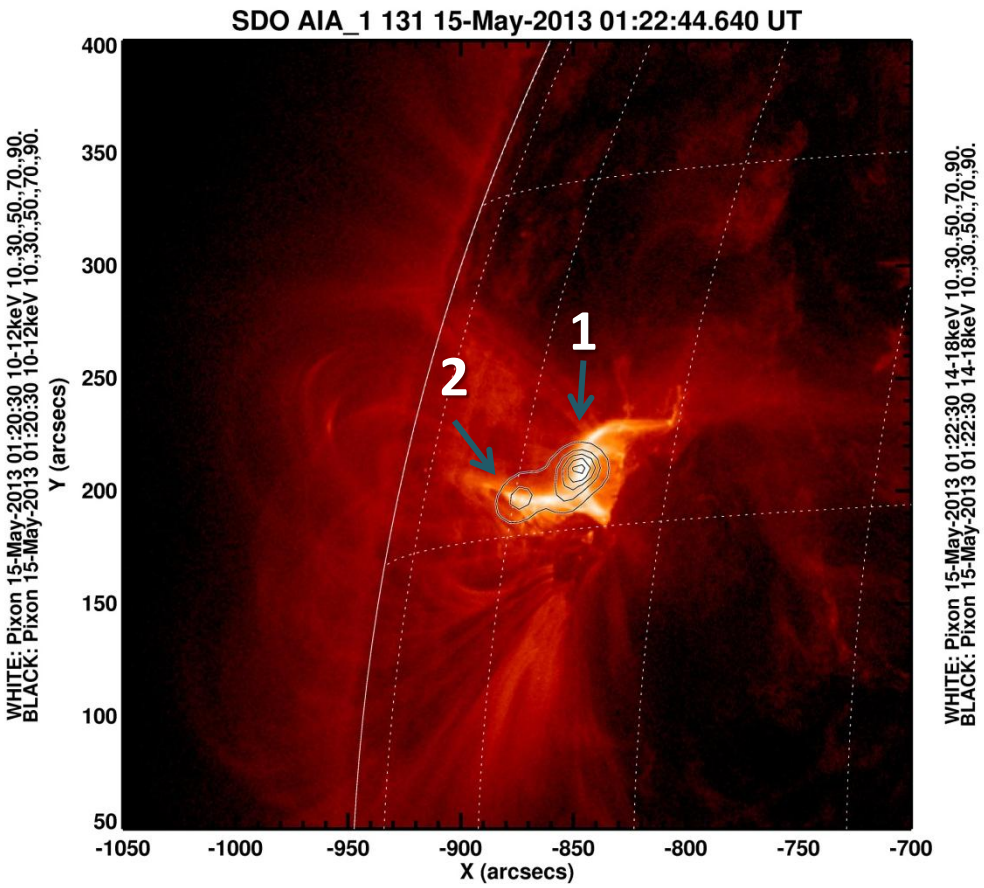

Top source of hard X-ray **no. 2** have been starting to dominate few seconds before the eruption of the nearest neighbouring loop

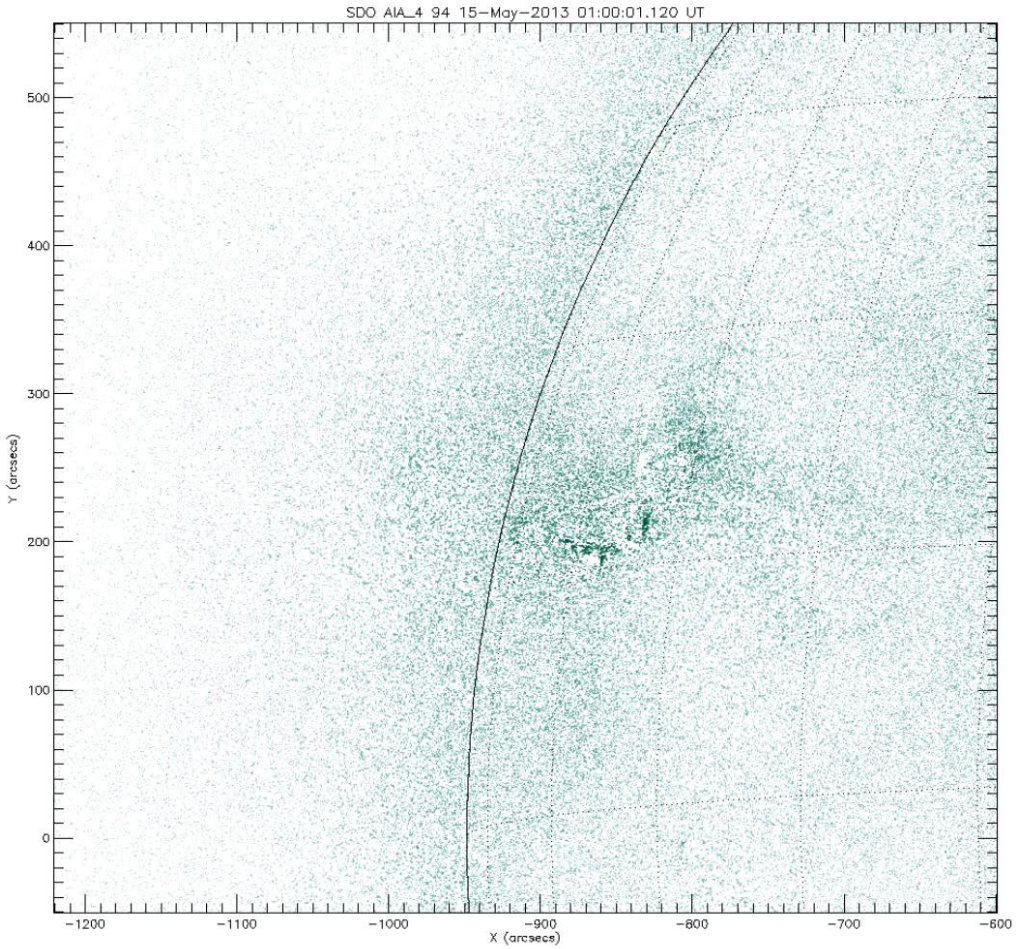

the animation of running different images in 94 Å (*SDO*/AIA)

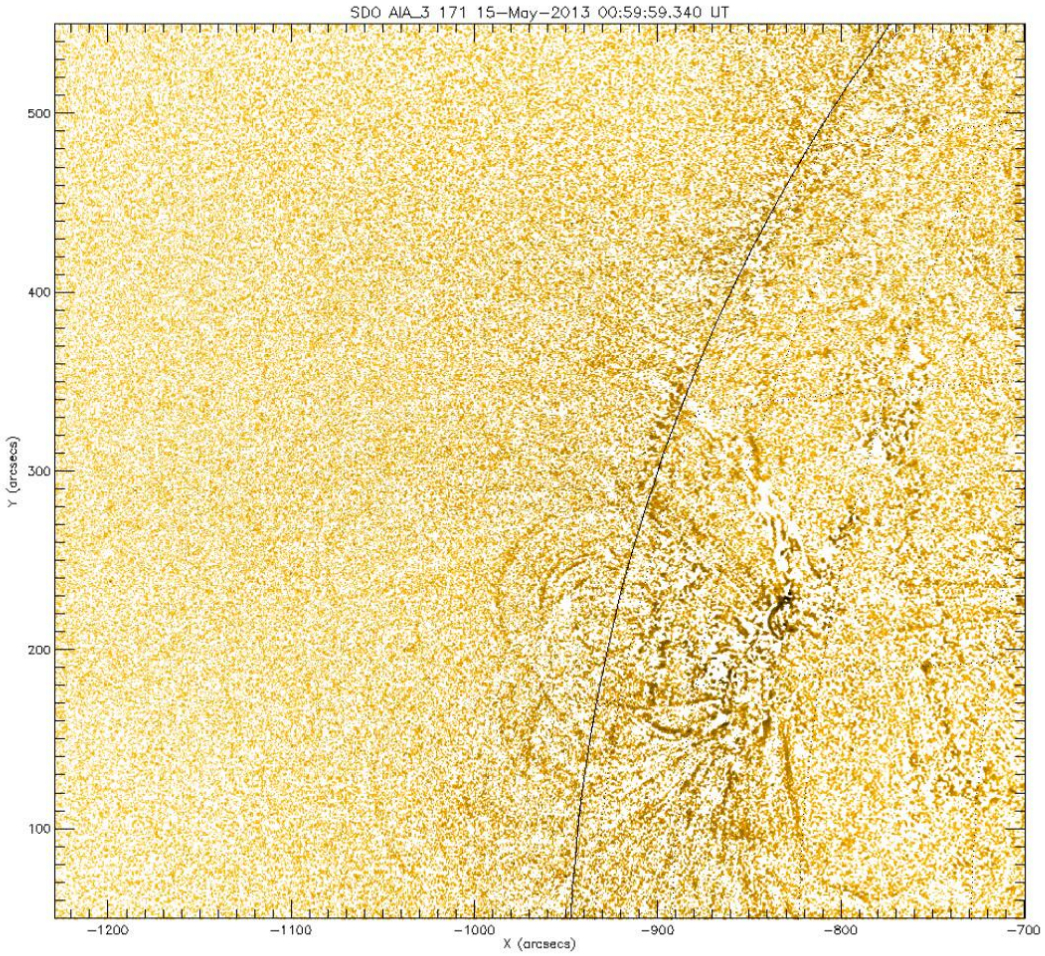

the animation of running different images in 171 Å (*SDO*/AIA)

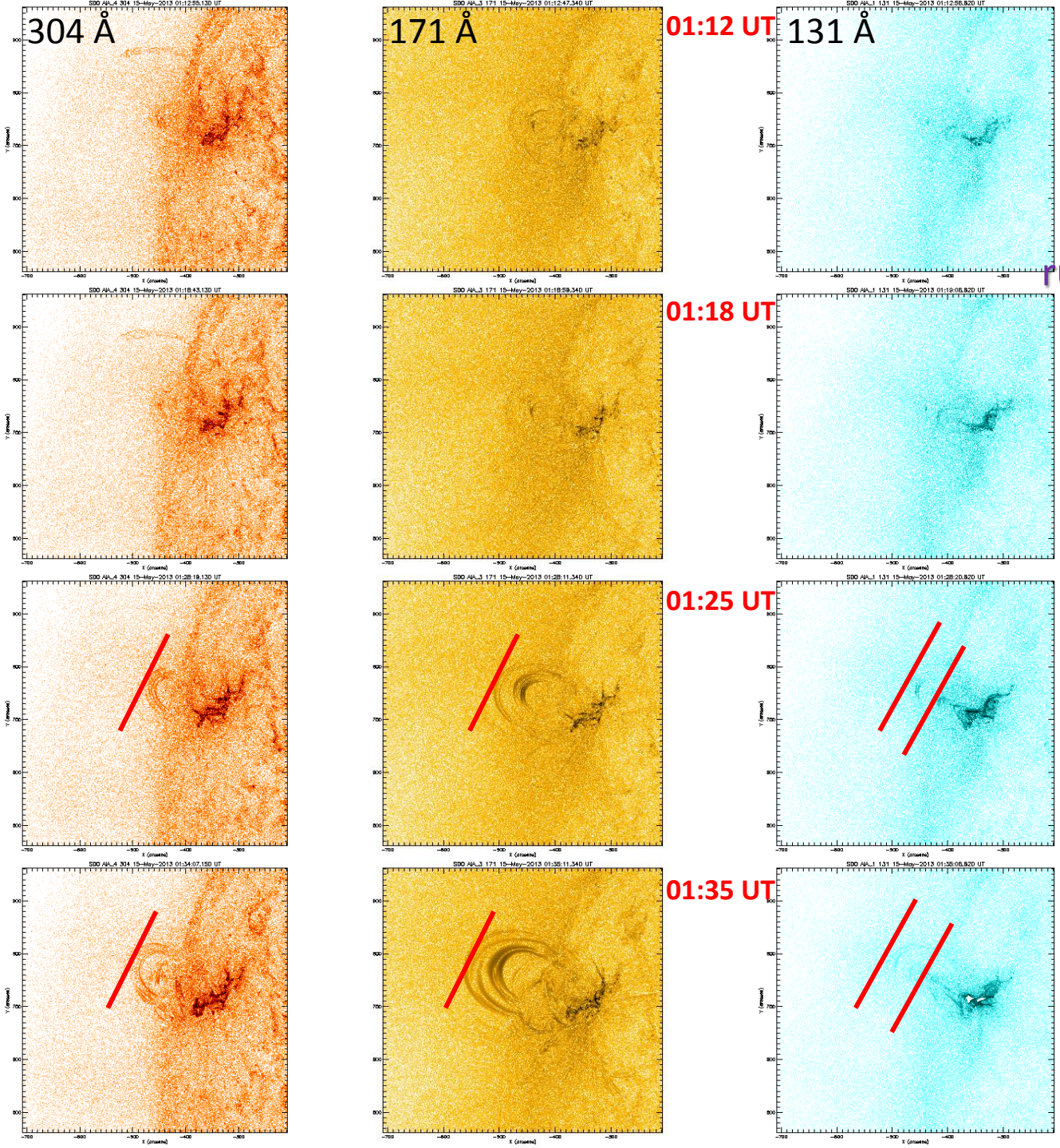

15.05.20

304Å (0.05 M

171Å (0.6 M

131Å (0.4 MK, 11 M

running difference imag

15 maja 2013-

temporal evolution of the brightness along the slice for 304 Å (0.05 MK) , 171 Å (0.6 MK) ,131 Å (0.4, 11 MK), 94 Å (7 MK)

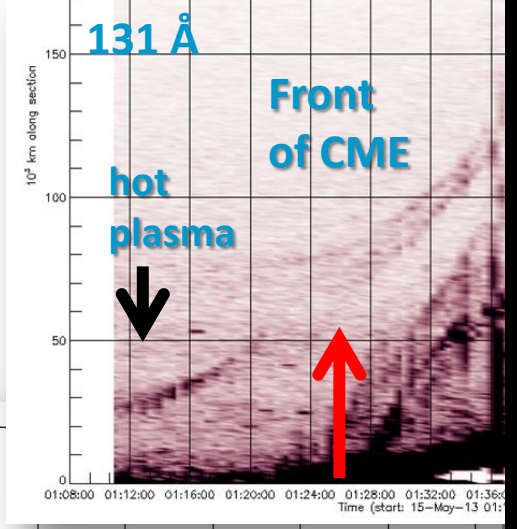

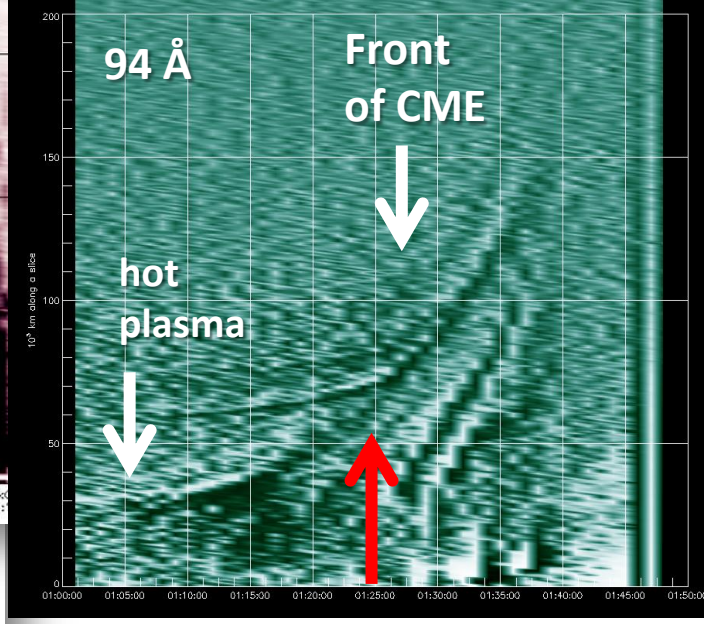

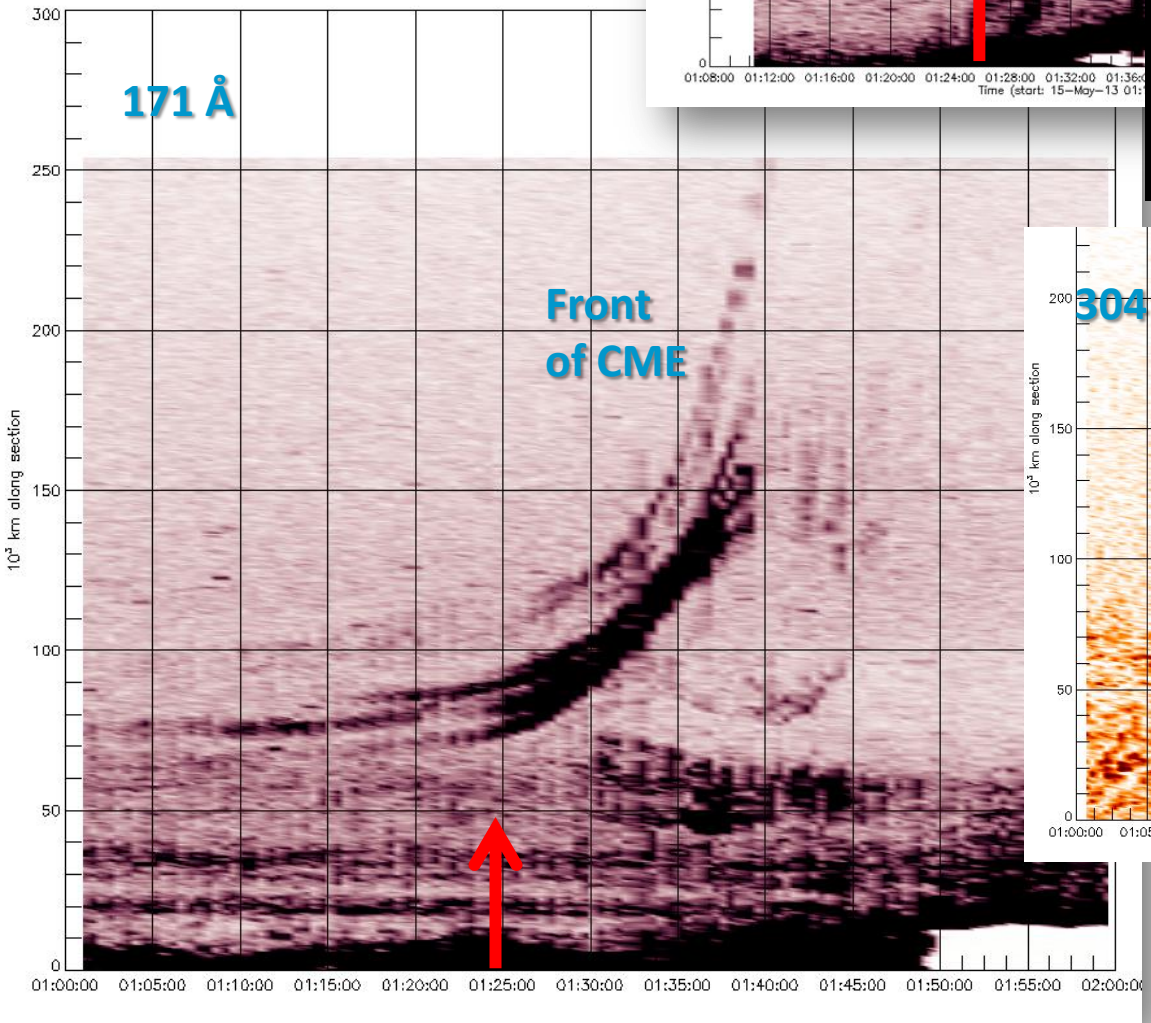

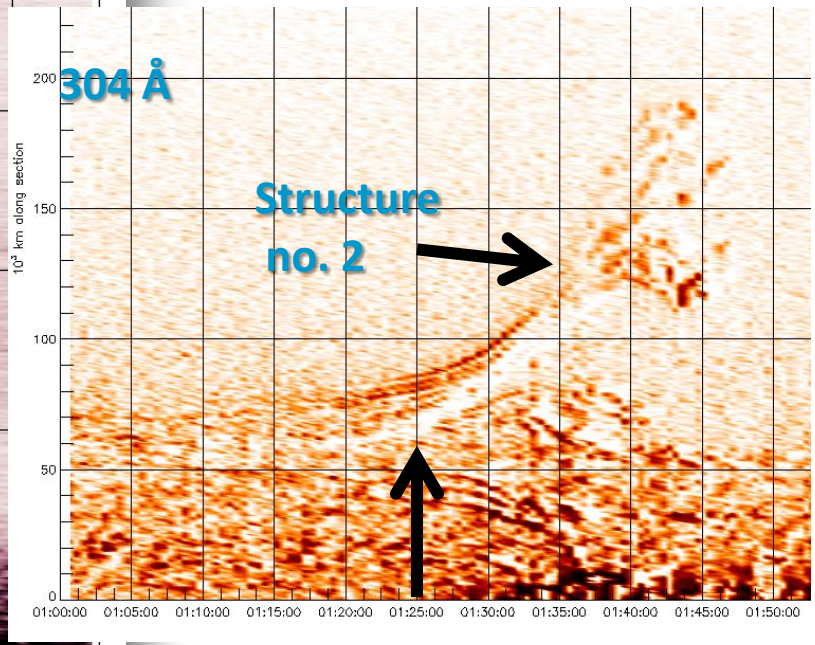

15 May 2013-

H(t) for 4 defined structures of CME observed in 131 Å, 171 Å i 304 Å AIA as well as *LASCO*/C2 i *LASCO*/C3

CME's leading edge, that were observed in 171 Å starts accelerating just before onset of flare .

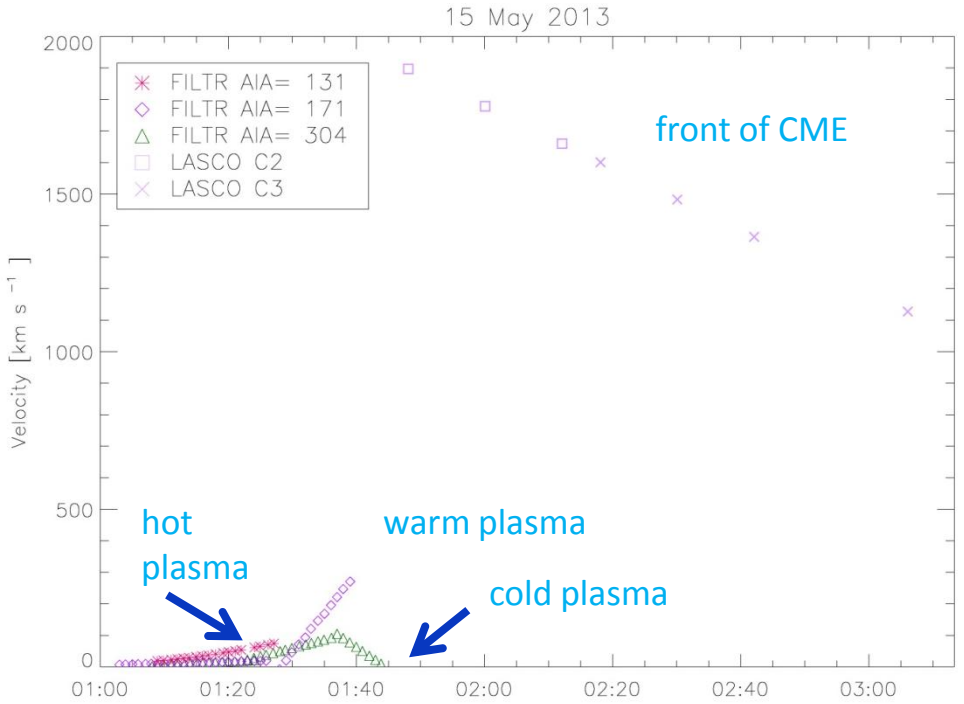

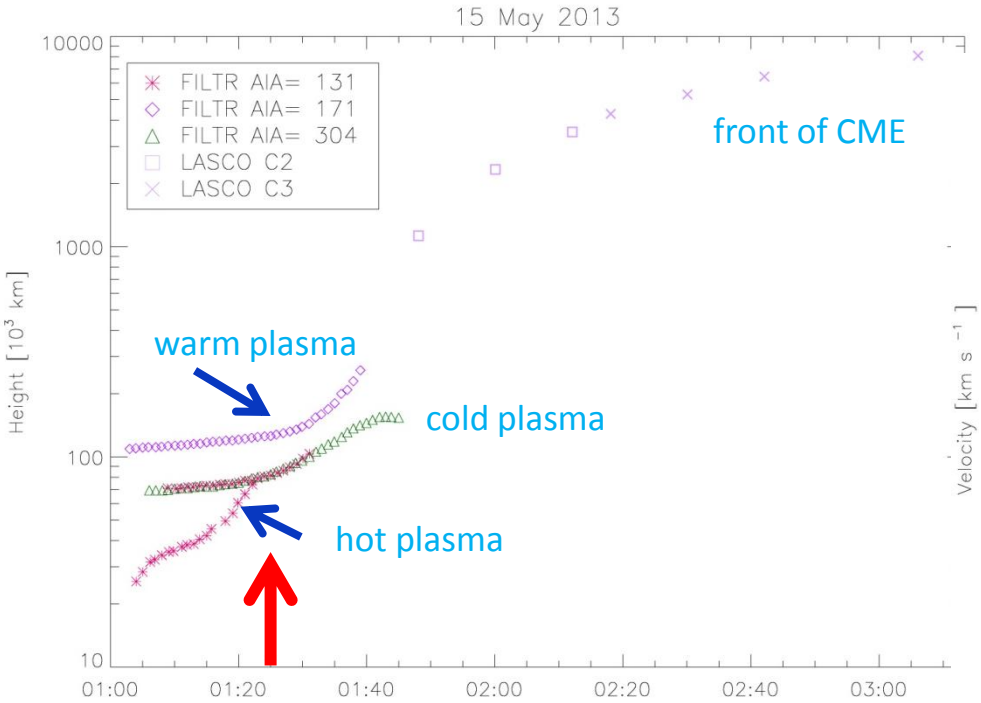

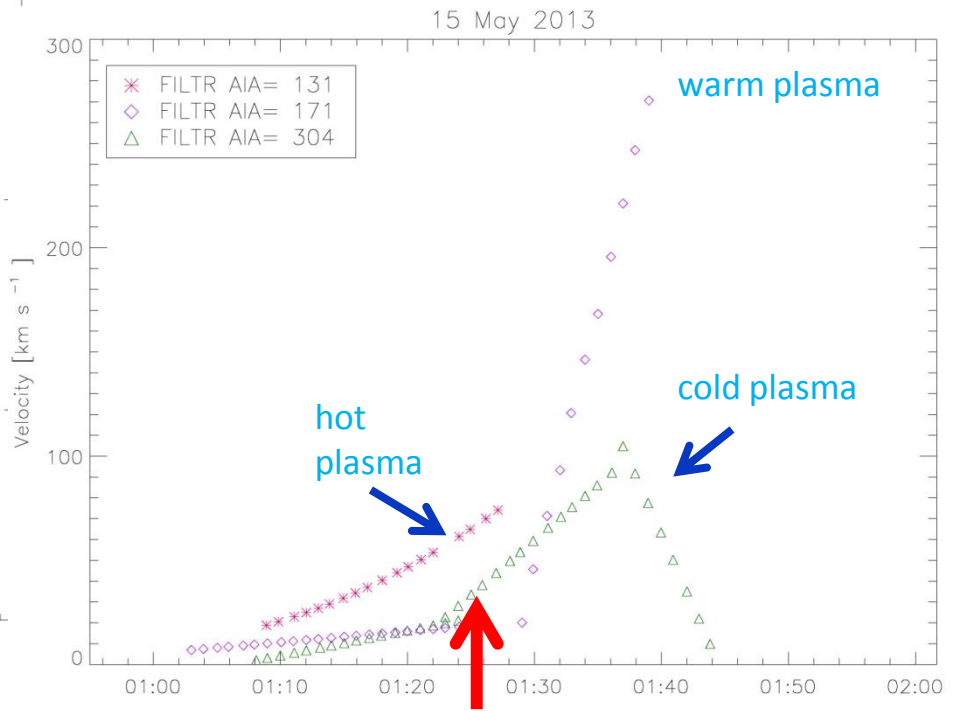

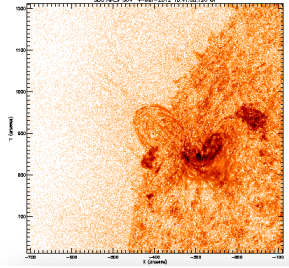

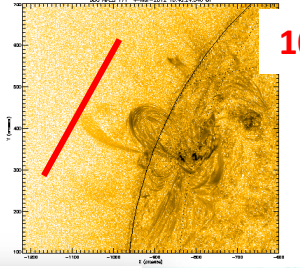

10:40 UT

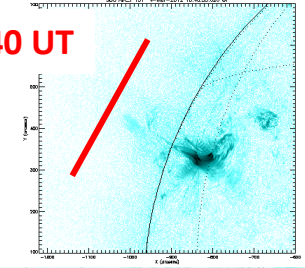

04 March 2012

304Å (0.05 MK), 171Å (0.6 MK),
131Å (0.4 MK, 11 MK)
running difference images

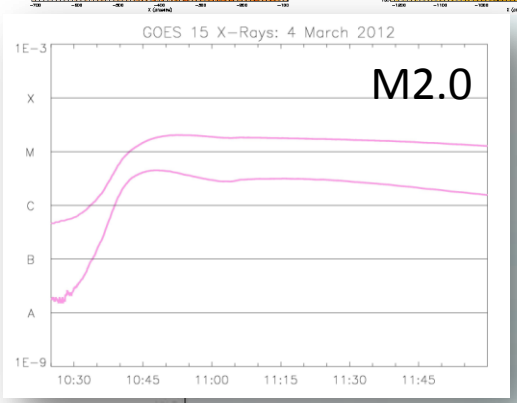

the animation of running different images in 131 Å (*SDO*/AIA)

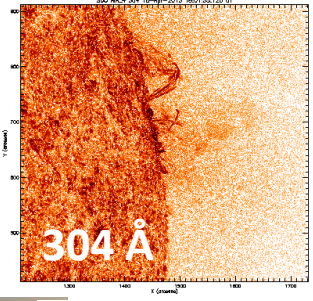

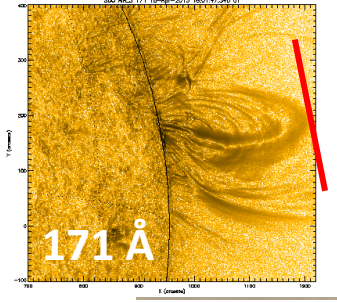

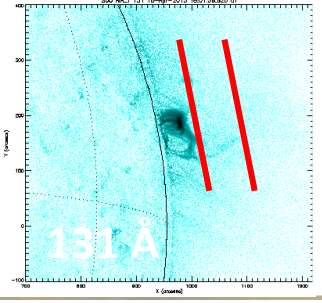

18 April 2013

304Å (0.05 MK), 171Å (0.6 MK),
131Å (0.4 MK, 11 MK)
running difference images

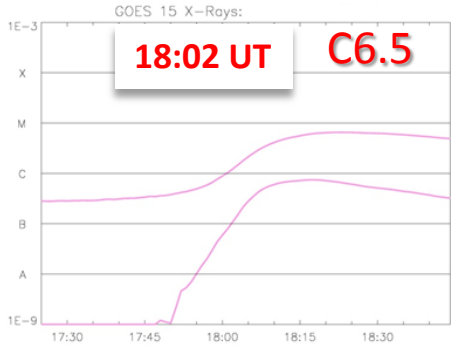

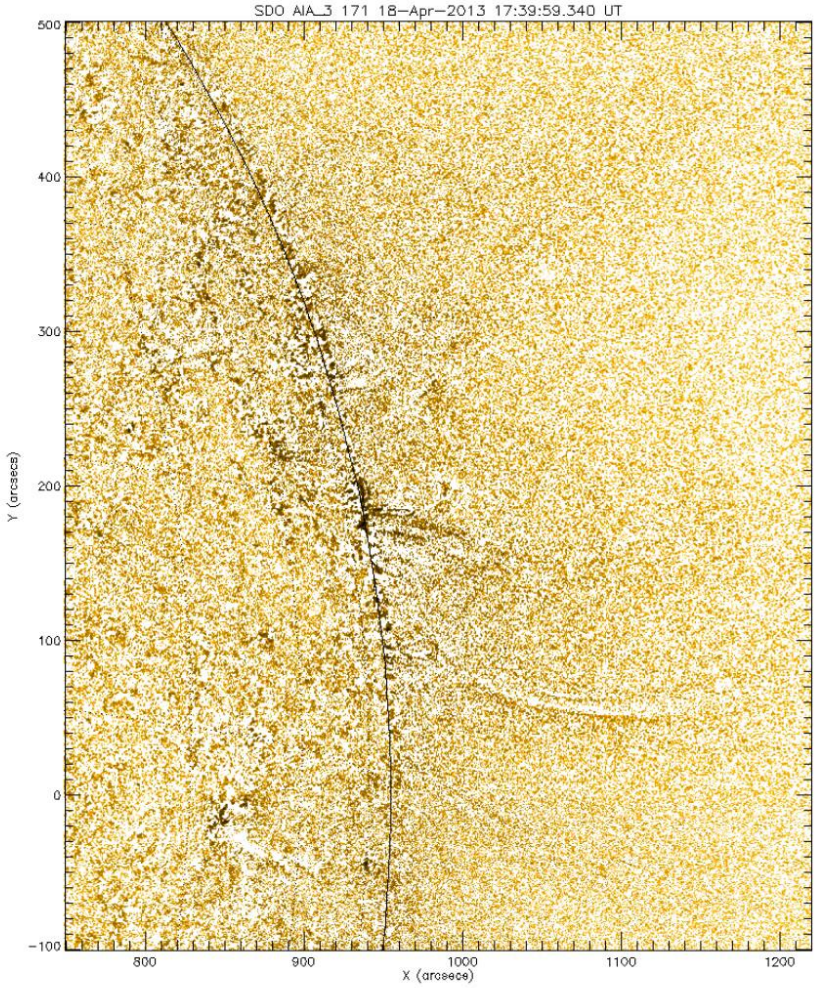

the animation of running different images in 171 Å (*SDO*/AIA)

H(t) and v(t) diagrams for two examples of eruptions

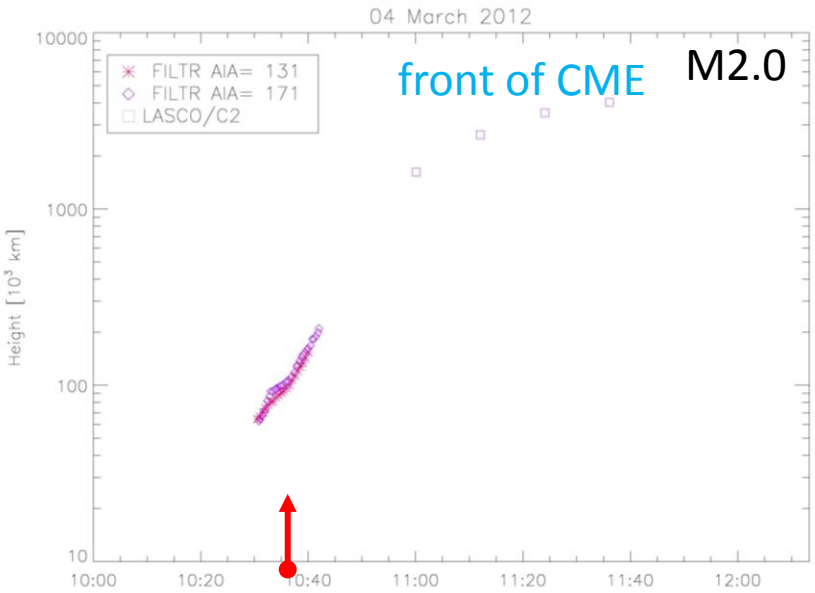

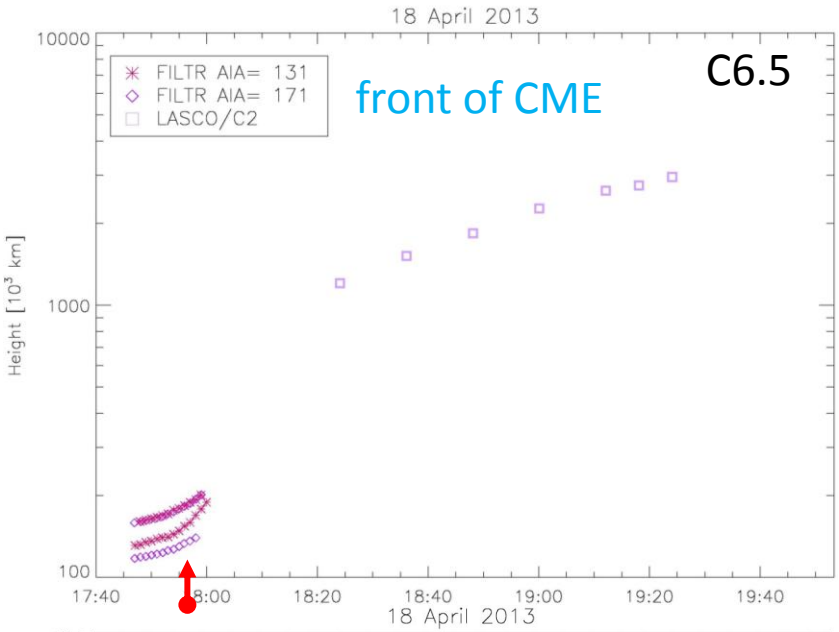

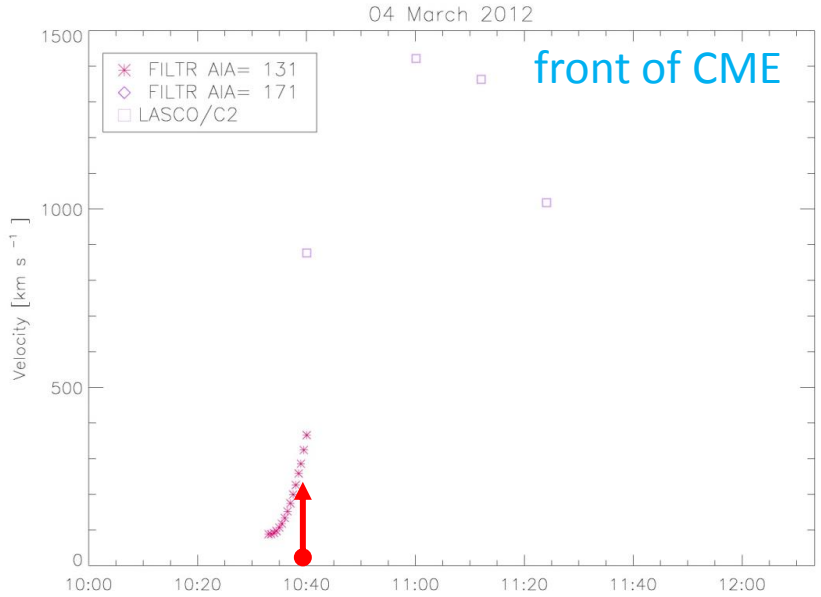

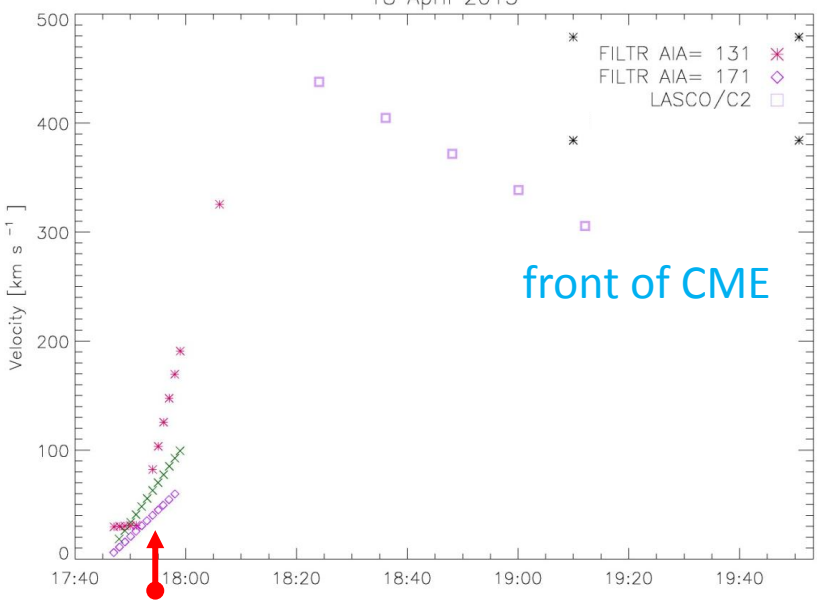

CME associated with eruptive prominences

For few examples we indentificated hot structures (seen in the high temperature passbands of the AIA), **before the impulsive acceleration phase of the eruption**.

In few cases we observed the kinematical scenario described by Zhang et al., 2001 (examples with the hot structure).

For CME associated with eruptive prominences we obtained lower speeds than for CME correlated with flares.

We noticed that in the case of CME associated with prominences we observed partial eruption.

18.04.2013- CME asssociated with prominence eruption

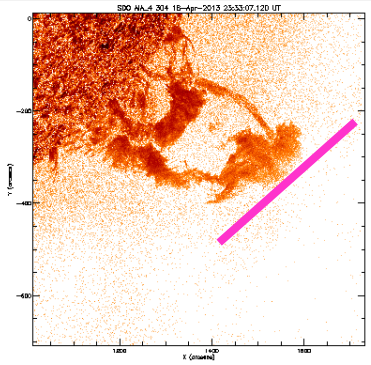

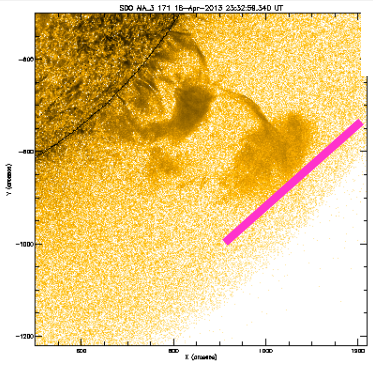

23:33 UT

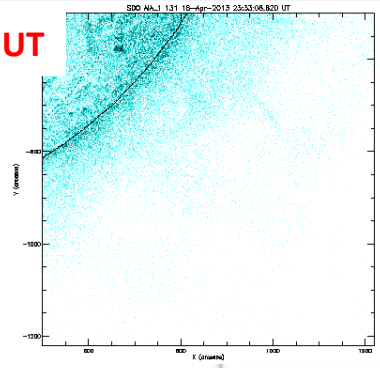

15.05.2013

304Å (0.05 MK),
171Å (0.6 MK),
131Å (0.4 MK, 11 MK)
running difference images

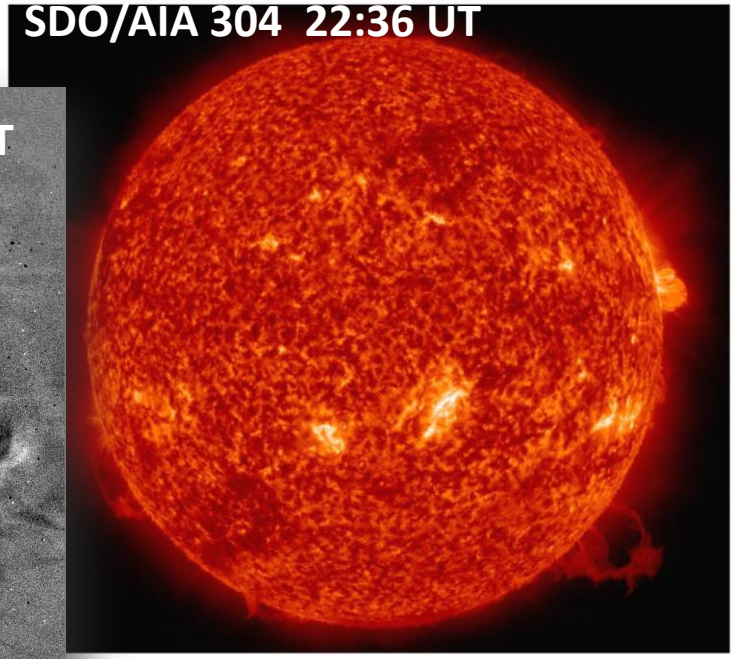

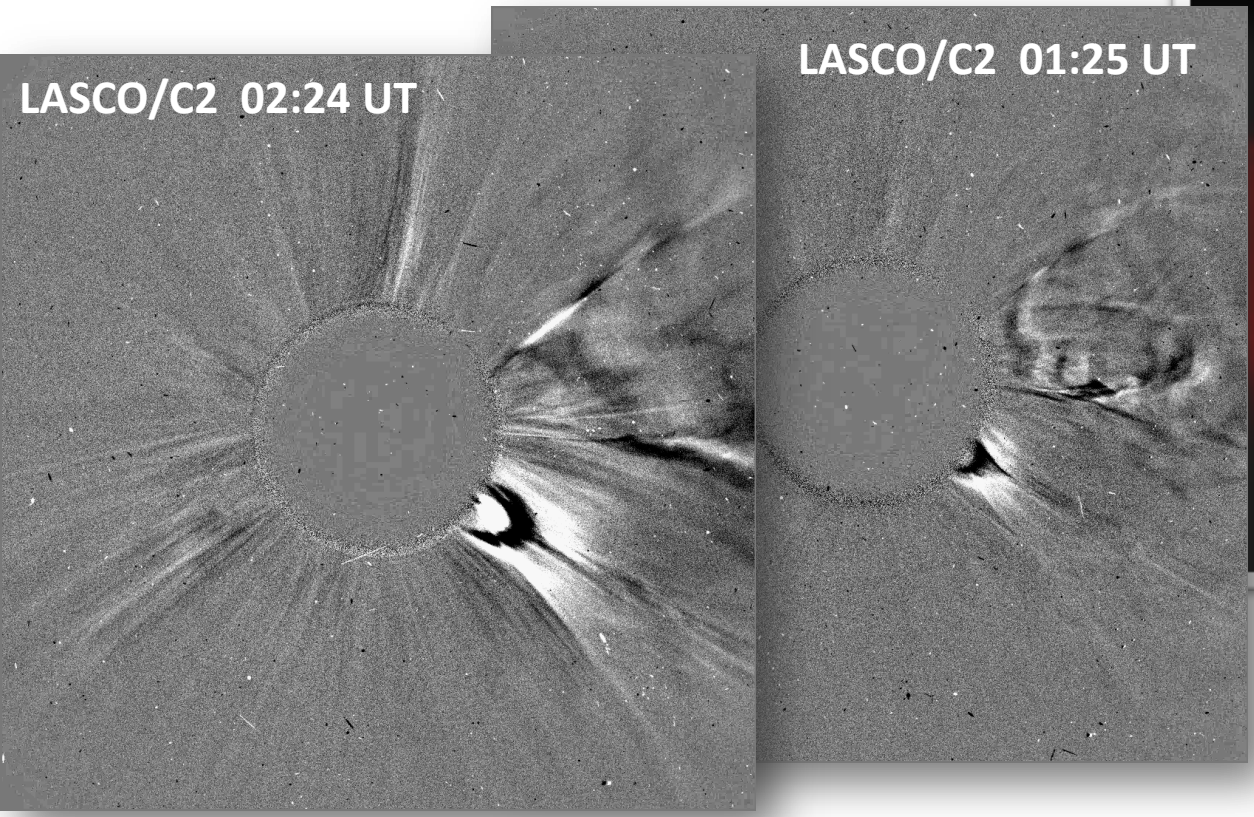

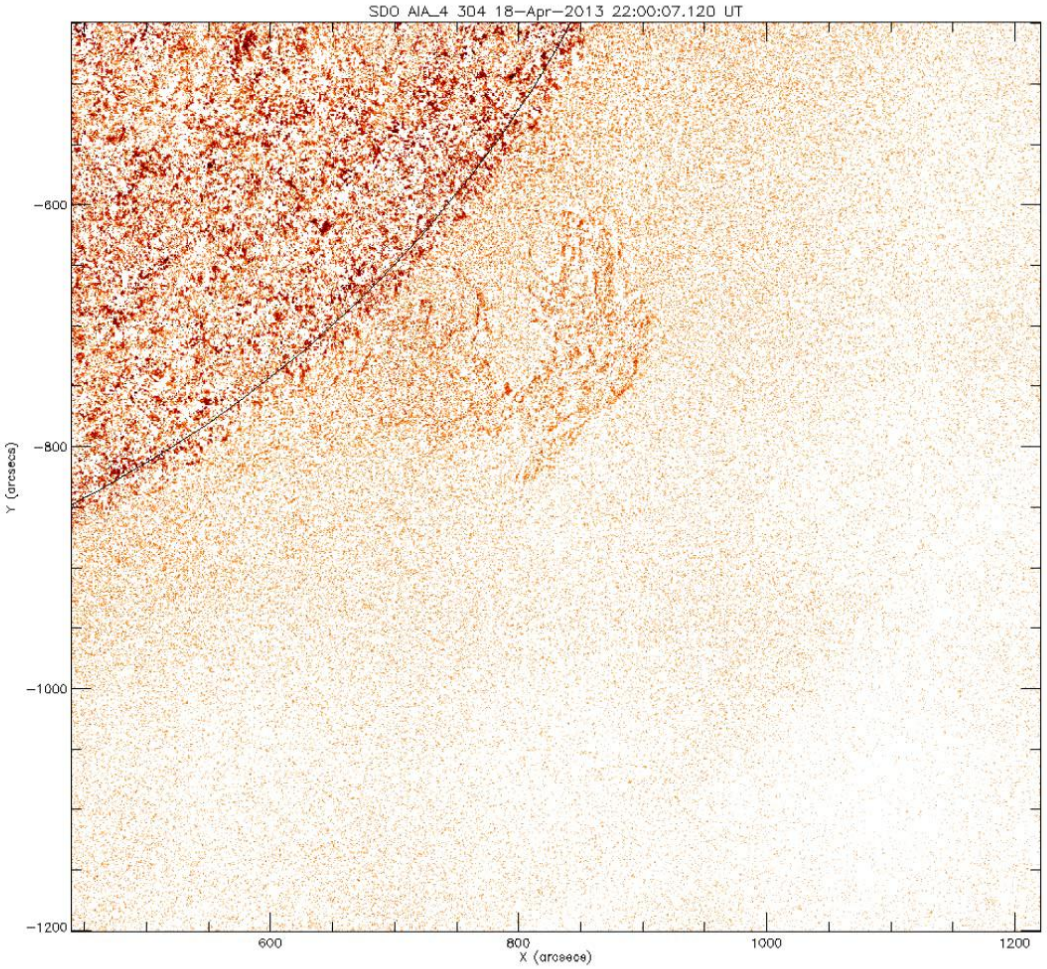

the animation of running different images in 304 Å (*SDO*/AIA)

18 April 2013-

temporal evolution of the brightness along the slice for **304 Å and H(t) were observed in 171 Å i 304 Å AIA i *LASCO*/C2**

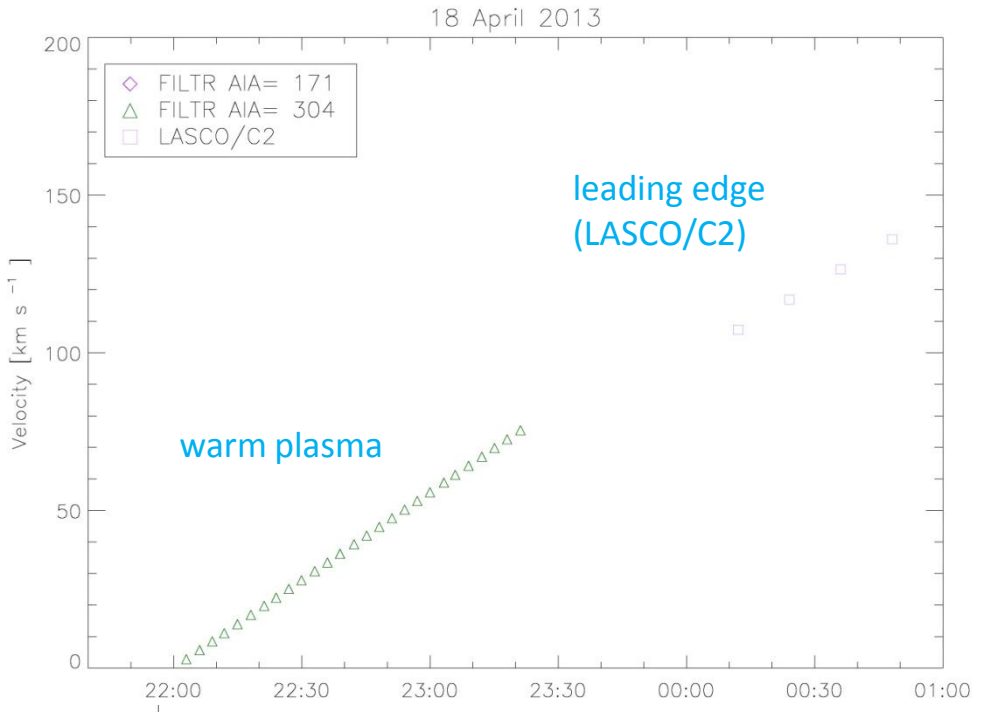

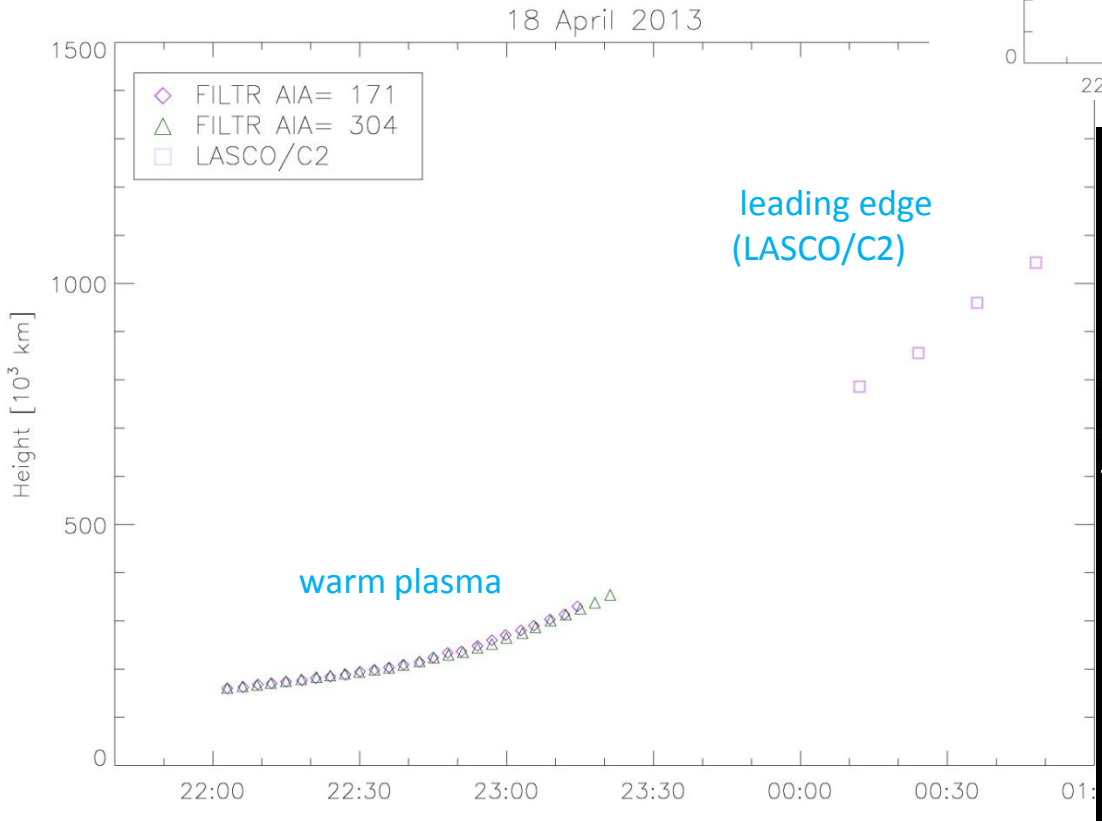

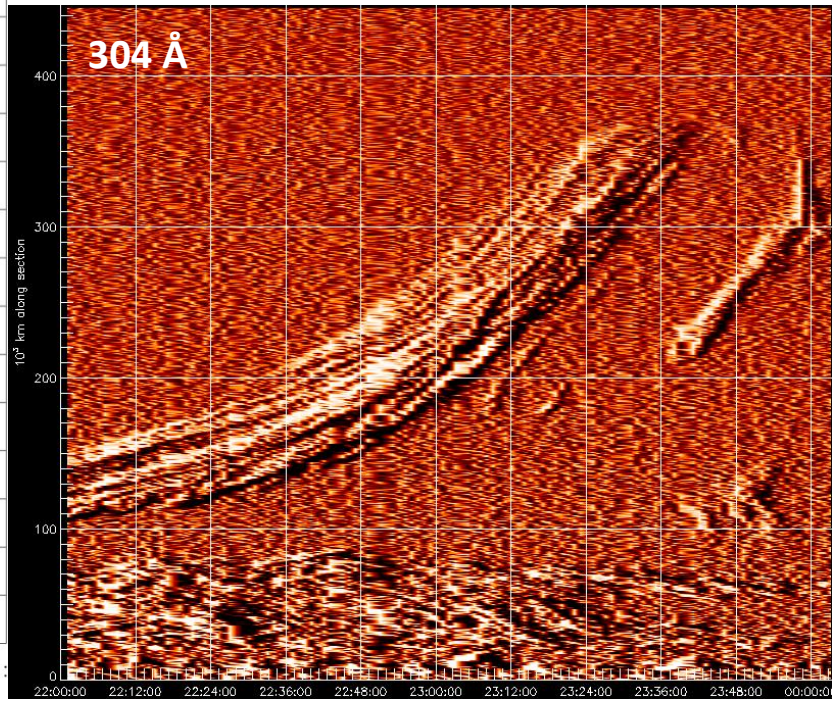

06.08.2013

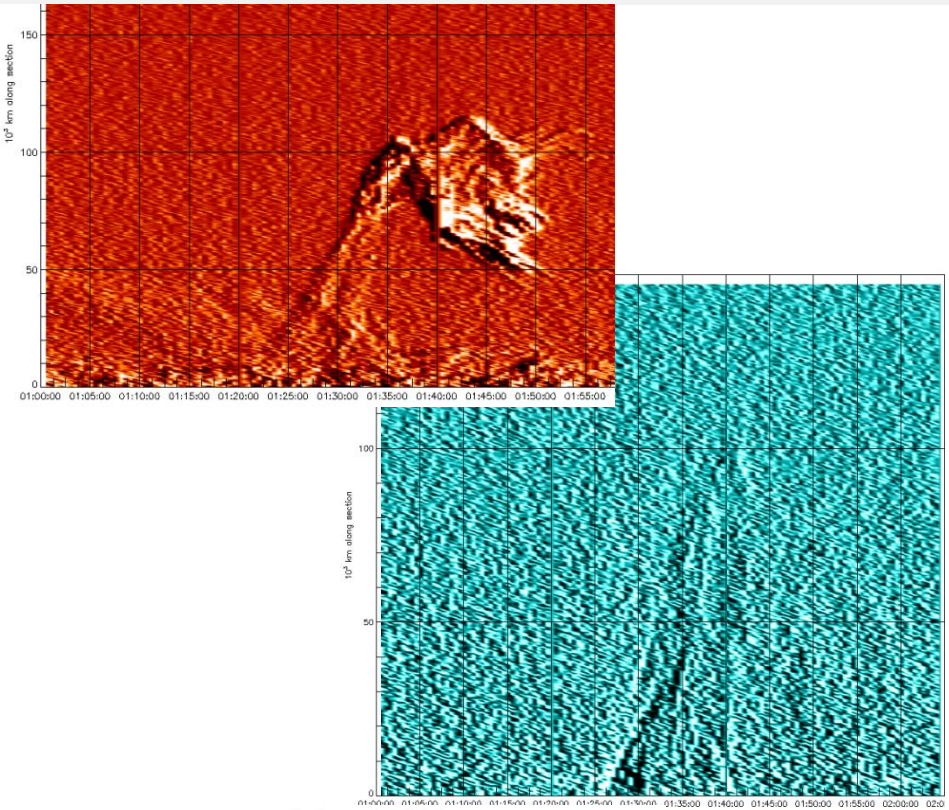

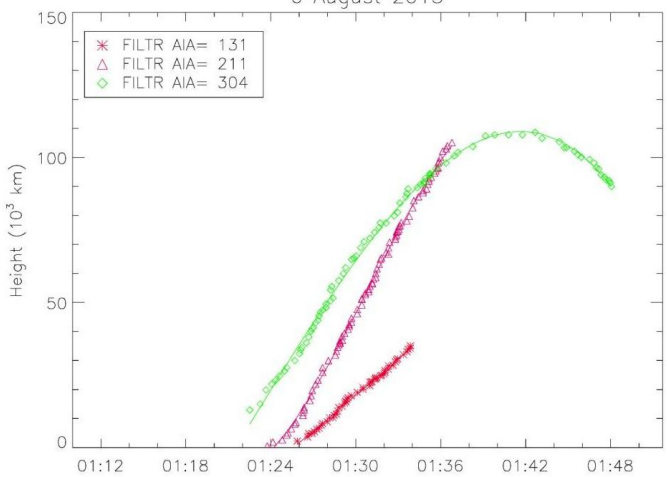

04.06.2013

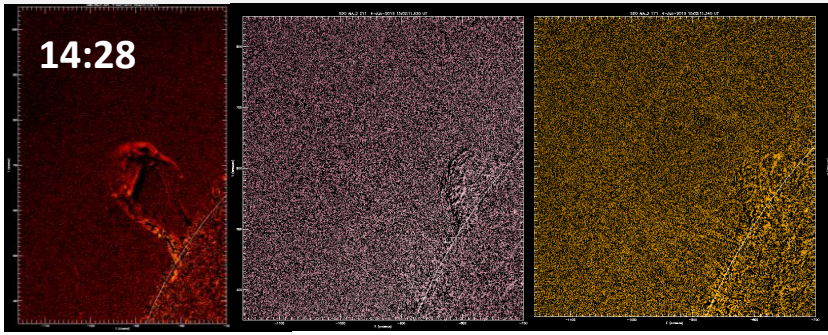

STEREO_B/SECCHI/EUVI 195

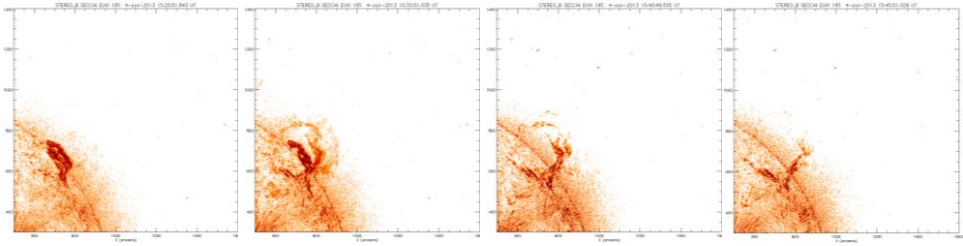

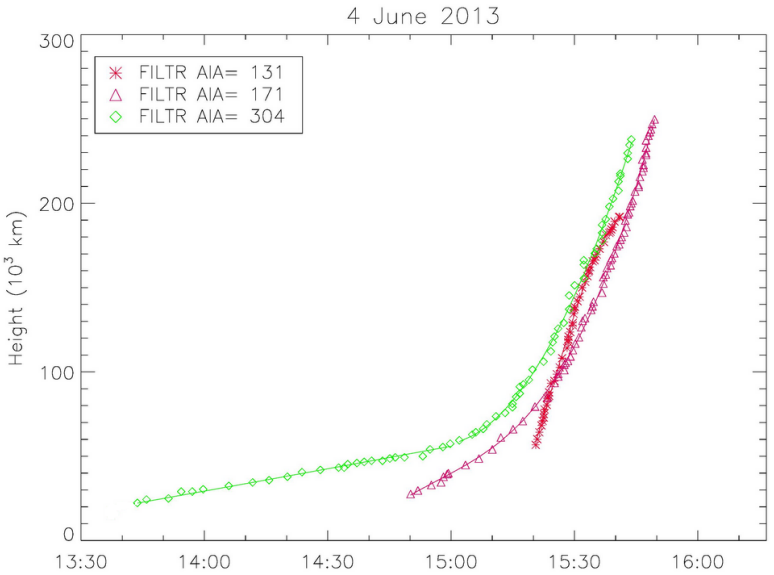

Conclusions:

- three phase kinematical scenario for F-CMEs
- higher speeds for F-CMEs
- hot structures or EUV post-flares loop for few NF-CMEs